Available on CMS information server

CMS NOTE-2007/032

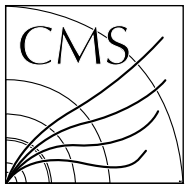

The Compact Muon Solenoid Experiment

CMS Note

Mailing address: CMS CERN, CH-1211 GENEVA 23, Switzerland

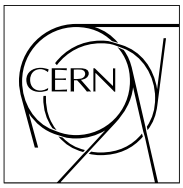

5 October 2007

Representation and Estimation of Trajectories from Two-body Decays

E. Widl, R. Fruhwirth

Abstract

A novel parametrization of the trajectories stemming from two-body decays is presented, based on the kinematics of the decay. The core component of this parametrization is a decay model which is derived using the relativistic energy-momentum conservation law and geometrical fundamentals. The estimation of the decay parameters, also including the beam profile and a mass constraint, is described. Some applications in realistics scenarios are presented. In addition, the representation of the trajectories for the use in track-based alignment algorithms is briefly discussed.

1 Introduction

The full information of reconstructed trajectories is usually concentrated in a set of five parameters for further analysis. Here, a novel parametrization of the trajectories stemming from a two-body decay is presented, based on the kinematics of such decays. This approach allows not only a compact representation, but also a direct estimation of the decay parameters. Furthermore, this representation is suitable for using the trajectories in a track-based alignment algorithm, due to the combined information content of the measurements and the superimposed physical constraints.

2 Prerequisites

The most fundamental prerequisite for tracking is the *track model* $\boldsymbol{f}$, that allows the representation of a set of measurements $\boldsymbol{m}$, belonging to a single track, by a set of parameters $\boldsymbol{q}$:

$$\boldsymbol{m} = \boldsymbol{f}(\boldsymbol{q}) + \boldsymbol{\epsilon}_m, \quad \mathsf{cov}(\boldsymbol{\epsilon}_m) = \boldsymbol{V}_m. \tag{1}$$

$\boldsymbol{\epsilon}_m$ is the stochastic deviation from the exact track model, containing both multiple scattering and measurement errors, and $\boldsymbol{V}_m$ is its variance-covariance matrix.

There exists a broad variety of possible sets of parameters [1] that in principle all come into question for the method descibed below. However, to simplify matters, it is assumed that the parameters $\boldsymbol{q}$ describe the *local state* of the trajectory at the surface of the first sensitive detector layer the particles traverse (see Figure 1). If the local coordinate system is Cartesian with axes (u, v, w), and the detector surface is defined by $w = 0$, a possible representation is $\boldsymbol{q} = (u, v, \mathrm{d}u/\mathrm{d}w, \mathrm{d}v/\mathrm{d}w, \kappa)^{\mathrm{T}}$, where κ is the curvature or the projected curvature. The track parameters at the other sensitive layers can be determined by propagating the initial state $\boldsymbol{q}$ through the magnetic field.

In the case of vertexing, another relation is of fundamental importance. Here, it is referred to as *measurement equation*, since it provides the connection between the observable and the primary physical and geometrical properties of a trajectory. The measurement equation expresses $\boldsymbol{q}$ as a function of the particle vertex $\boldsymbol{v}$ and its momentum at the vertex $\boldsymbol{p}_v$:

$$\boldsymbol{q} = \boldsymbol{q}(\boldsymbol{v}, \boldsymbol{p}_v). \tag{2}$$

Of course also quantities like the magnetic field in the tracking volume or the mass of the particle are a necessary input to the track model and the measurement equation. Nevertheless, it can be assumed that they are known and remain the same for all tracks (of the same kind) and are therefore not treated as free parameters.

3 Parametrization

Consider the decay of a primary particle with mass M and momentum $\boldsymbol{p}$ into a particle-antiparticle pair. The momenta $\boldsymbol{p}^{\pm}_{\text{c.m.s.}}$ of the secondary particles in the center-of-mass system of this two-body decay, i.e. the rest frame of the primary particle, can be be obtained using the relativistic energy-momentum conservation law:

$$\boldsymbol{p}^{\pm}_{\text{c.m.s.}} = \pm m\sqrt{\alpha^2 - 1} \begin{pmatrix} \sin\theta\,\cos\phi \\ \sin\theta\,\sin\phi \\ \cos\theta \end{pmatrix} \tag{3}$$

where m is the mass of the secondary particles and $\alpha = \frac{M}{2m}$.

At this point a convention is needed that defines the direction of the coordinate axes in the rest frame of the primary particle (X, Y, Z) with respect to the lab-frame (x, y, z), in order to provide a proper definition of the polar angle $\theta \in [0, \pi]$ and the azimuth angle $\phi \in [0, 2\pi)$. Here, the Z-axis was chosen to coincide with the direction of the primary particle momentum $\boldsymbol{p} = (p_x, p_y, p_z)^{\mathrm{T}}$ in the lab frame. The X- and Y-axis were chosen to coincide with the x- and y-axis after subsequent rotations around the z-axis by $\tan\gamma = p_y/p_x$ (clockwise) and the y-axis by $\tan\beta = p_z/p_{\mathrm{T}}$ (counter-clockwise, with $p_{\mathrm{T}}^2 = p_x^2 + p_y^2$). See Figure 2 for a schematic view of the relative positions of these frames.

By doing so, the momenta only have to be boosted along the Z-axis and properly rotated to obtain the lab-frame representation. The resulting *decay model* correlates the momenta of both secondary particles to a single set of

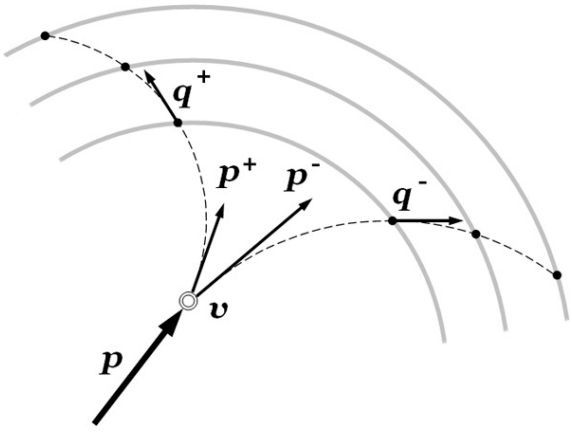

Figure 1: Schematic view of the decay. The dashed lines represent the trajectories, the detector layers are sketched by bold grey lines.

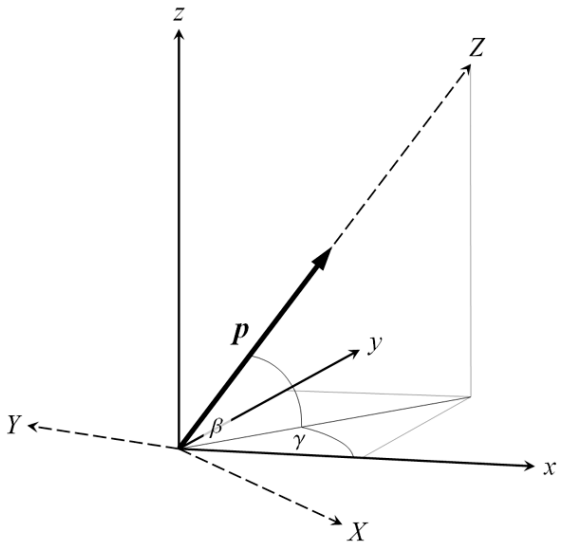

Figure 2: Relative position of the lab-frame (x, y, z) and the rest-frame (X, Y, Z) of the primary particle with momentum $\boldsymbol{p}$.

kinematical parameters ($p = |\boldsymbol{p}|$):

$$\boldsymbol{p}^{\pm}(p_x, p_y, p_z, \theta, \phi, M) = \begin{pmatrix} \frac{p_x p_z}{p_{\mathrm{T}} p} & -\frac{p_y}{p_{\mathrm{T}}} & \frac{p_x}{p} \\ \frac{p_y p_z}{p_{\mathrm{T}} p} & \frac{p_x}{p_{\mathrm{T}}} & \frac{p_y}{p} \\ -\frac{p_{\mathrm{T}}}{p} & 0 & \frac{p_z}{p} \end{pmatrix} \begin{pmatrix} \pm m\sqrt{\alpha^2 - 1}\, \sin\theta\, \cos\phi \\ \pm m\sqrt{\alpha^2 - 1}\, \sin\theta\, \sin\phi \\ \frac{p}{2} \pm \frac{1}{2}\sqrt{\frac{\alpha^2 - 1}{\alpha^2}\,(p^2 + M^2)}\, \cos\theta \end{pmatrix} \tag{4}$$

Note that the superscript indices $+$ and $-$ refer to the signs in Eq. (3) and not to the charge of the daughter particles.

Considering what was said above about the track model and the measurement equation it follows that in the case of two-body decays of the form $\mathrm{X}^0 \longrightarrow \mathrm{Y}^+\mathrm{Y}^-$, the use of the decay model allows to represent the corresponding trajectories by the following 9 parameters:

1. the position of the decay vertex $\boldsymbol{v} = (v_x, v_y, v_z)^T$,
2. the momentum of the primary particle $\boldsymbol{p} = (p_x, p_y, p_z)^T$ in the lab-frame,
3. the polar angle θ and the azimuth angle ϕ defining the direction of the secondary particles in the rest-frame of the primary particle, and
4. the mass M of the primary particle.

4 Representation

The full set of parameters defining the kinematic properties are from now on denoted with $\boldsymbol{z} = (p_x, p_y, p_z, \theta, \phi, M)$. The information fed for instance to an alignment algorithm then takes the following form:

$$\boldsymbol{m} = \begin{pmatrix} \boldsymbol{m}^+ \\ \boldsymbol{m}^- \end{pmatrix} = \begin{pmatrix} \boldsymbol{f}^+(\boldsymbol{v}, \boldsymbol{z}) + \boldsymbol{\epsilon}_m^+ \\ \boldsymbol{f}^-(\boldsymbol{v}, \boldsymbol{z}) + \boldsymbol{\epsilon}_m^- \end{pmatrix}, \qquad \boldsymbol{V}_m = \begin{pmatrix} \boldsymbol{V}_m^+ & \boldsymbol{\emptyset} \\ \boldsymbol{\emptyset} & \boldsymbol{V}_m^- \end{pmatrix},$$

$$\boldsymbol{D} = \frac{\partial \boldsymbol{f}}{\partial(\boldsymbol{v}, \boldsymbol{z})} = \begin{pmatrix} \frac{\partial \boldsymbol{f}^+}{\partial \boldsymbol{q}^+} \cdot \frac{\partial \boldsymbol{q}^+}{\partial \boldsymbol{v}} & \frac{\partial \boldsymbol{f}^+}{\partial \boldsymbol{q}^+} \cdot \frac{\partial \boldsymbol{q}^+}{\partial \boldsymbol{p}^+} \cdot \frac{\partial \boldsymbol{p}^+}{\partial \boldsymbol{z}} \\ \frac{\partial \boldsymbol{f}^-}{\partial \boldsymbol{q}^-} \cdot \frac{\partial \boldsymbol{q}^-}{\partial \boldsymbol{v}} & \frac{\partial \boldsymbol{f}^+}{\partial \boldsymbol{q}^-} \cdot \frac{\partial \boldsymbol{q}^-}{\partial \boldsymbol{p}^-} \cdot \frac{\partial \boldsymbol{p}^-}{\partial \boldsymbol{z}} \end{pmatrix}$$

Here $\boldsymbol{m}^{\pm}$ and $\boldsymbol{V}^{\pm}$ are the measurements and the corresponding covariance matrices of the single trajectories. In the derivative matrix $\boldsymbol{D}$ the chain rule is used, combining the Jacobians $\partial \boldsymbol{f}^{\pm}/\partial \boldsymbol{q}$ with the Jacobians of the measurement equation $\boldsymbol{q}(\boldsymbol{v}, \boldsymbol{p}_v)$ and the decay model $\boldsymbol{p}^{\pm}(\boldsymbol{z})$.

5 Estimation

5.1 General χ^2 Solution

The *estimated* single-track parameters $\boldsymbol{q}^{\pm}_{\text{est}}$ are related to the true vertex position $\boldsymbol{v}$ and the true momentum of the particle at the vertex $\boldsymbol{p}^{\pm}$ via the measurement equation $\boldsymbol{q}(\boldsymbol{v}, \boldsymbol{p}_v)$:

$$\begin{pmatrix} \boldsymbol{q}^{+}_{\text{est}} \\ \boldsymbol{q}^{-}_{\text{est}} \end{pmatrix} = \begin{pmatrix} \boldsymbol{q}(\boldsymbol{v}, \boldsymbol{p}^{+}) \\ \boldsymbol{q}(\boldsymbol{v}, \boldsymbol{p}^{-}) \end{pmatrix} + \begin{pmatrix} \boldsymbol{\epsilon}^{+} \\ \boldsymbol{\epsilon}^{-} \end{pmatrix}, \quad \mathsf{cov}(\boldsymbol{\epsilon}^{\pm}) = \boldsymbol{V}^{\pm} = (\boldsymbol{W}^{\pm})^{-1}.$$

Using a first-order Taylor expansion at the expansion point $\boldsymbol{v}_0 = (v_{0x}, v_{0y,v_{0z}})^{\mathrm{T}}$ and $\boldsymbol{z}_0 = (p_{0x}, p_{0y}, p_{0z}, \theta_0, \phi_0, M_0)^{\mathrm{T}}$ this relation can be linearized:

$$\begin{pmatrix} \boldsymbol{q}^{+}_{\text{est}} \\ \boldsymbol{q}^{-}_{\text{est}} \end{pmatrix} = \begin{pmatrix} \boldsymbol{c}^{+} \\ \boldsymbol{c}^{-} \end{pmatrix} + \begin{pmatrix} \boldsymbol{A}^{+} & \boldsymbol{B}^{+} & \boldsymbol{\emptyset} \\ \boldsymbol{A}^{-} & \boldsymbol{\emptyset} & \boldsymbol{B}^{-} \end{pmatrix} \begin{pmatrix} \boldsymbol{v} \\ \boldsymbol{p}^{+} \\ \boldsymbol{p}^{-} \end{pmatrix} + \begin{pmatrix} \boldsymbol{\epsilon}^{+} \\ \boldsymbol{\epsilon}^{-} \end{pmatrix}$$

where

$$\boldsymbol{A}^{\pm} = \partial \boldsymbol{q} / \partial \boldsymbol{v}\big|_{\boldsymbol{v}_0\,, \boldsymbol{p}^{\pm}_0}, \qquad \boldsymbol{B}^{\pm} = \partial \boldsymbol{q} / \partial \boldsymbol{p}\big|_{\boldsymbol{v}_0\,, \boldsymbol{p}^{\pm}_0},$$
$$\boldsymbol{c}^{\pm} = \boldsymbol{q}(\boldsymbol{v}_0\,, \boldsymbol{p}^{\pm}_0) - \boldsymbol{A}^{\pm}\boldsymbol{v}_0 - \boldsymbol{B}^{\pm}\boldsymbol{p}^{\pm}_0, \qquad \boldsymbol{p}^{\pm}_0 = \boldsymbol{p}^{\pm}(\boldsymbol{z}_0\,).$$

It should be noted that this linearization is the standard approach for vertexing. For this reason, the computation of the matrices $\boldsymbol{A}^{\pm}$ and $\boldsymbol{B}^{\pm}$ is always provided in an actual implementation.

Since the momenta of the secondary particles depend on the same set of parameters, the linearization of the decay model (4),

$$\boldsymbol{p}^{\pm}(\boldsymbol{z}) = \boldsymbol{d}^{\pm} + \boldsymbol{C}^{\pm}\boldsymbol{z}$$

with

$$\boldsymbol{C}^{\pm} = \partial \boldsymbol{p}^{\pm} / \partial \boldsymbol{z}\big|_{\boldsymbol{z}_0} \quad \text{and} \quad \boldsymbol{d}^{\pm} = \boldsymbol{p}^{\pm}_0 - \boldsymbol{C}^{\pm}\boldsymbol{z}_0\,,$$

can be used to rewrite the equations as:

$$\begin{pmatrix} \boldsymbol{q}^{+}_{\text{est}} - \boldsymbol{c}^{+} - \boldsymbol{B}^{+}\boldsymbol{d}^{+} \\ \boldsymbol{q}^{-}_{\text{est}} - \boldsymbol{c}^{-} - \boldsymbol{B}^{-}\boldsymbol{d}^{-} \end{pmatrix} = \begin{pmatrix} \boldsymbol{A}^{+} & \boldsymbol{B}^{+}\boldsymbol{C}^{+} \\ \boldsymbol{A}^{-} & \boldsymbol{B}^{-}\boldsymbol{C}^{-} \end{pmatrix} \begin{pmatrix} \boldsymbol{v} \\ \boldsymbol{z} \end{pmatrix} + \begin{pmatrix} \boldsymbol{\epsilon}^{+} \\ \boldsymbol{\epsilon}^{-} \end{pmatrix}$$

These 10 linear equations allow to make an estimate on the vertex position (3 parameters) and the kinematical properties (6 parameters). It should be noted that this approach avoids the use of Lagrange multipliers; instead the kinematical constraints are enforced by incorporating the kinematics in the decay model. Hence the straightforward treatment of these equations within a general χ^2 minimization of the residuals, i.e. the minimization of the objective function

$$\chi^2(\boldsymbol{v}, \boldsymbol{z}) = \sum_{i=\pm} \left(\boldsymbol{r}^i - \boldsymbol{s}^i(\boldsymbol{v}, \boldsymbol{z})\right)^{\mathrm{T}} \boldsymbol{W}^i \left(\boldsymbol{r}^i - \boldsymbol{s}^i(\boldsymbol{v}, \boldsymbol{z})\right) \longrightarrow \min$$

with

$$\boldsymbol{r}^{\pm} = \boldsymbol{q}^{\pm}_{\text{est}} - \boldsymbol{c}^{+} - \boldsymbol{B}^{\pm}\boldsymbol{d}^{\pm}, \quad \boldsymbol{s}^{\pm}(\boldsymbol{v}, \boldsymbol{z}) = \boldsymbol{A}^{\pm}\boldsymbol{v} + \boldsymbol{B}^{\pm}\boldsymbol{C}^{\pm}\boldsymbol{z},$$

yields the following estimates [2]:

$$\begin{pmatrix} \tilde{\boldsymbol{v}} \\ \tilde{\boldsymbol{z}} \end{pmatrix} = \operatorname{argmin} \chi^2(\boldsymbol{v}, \boldsymbol{z}) = (\boldsymbol{J}^{\mathrm{T}}\boldsymbol{W}\boldsymbol{J})^{-1}\boldsymbol{J}^{\mathrm{T}}\boldsymbol{W}\boldsymbol{r} \tag{5}$$

with

$$\boldsymbol{r} = \begin{pmatrix} \boldsymbol{r}^{+} \\ \boldsymbol{r}^{-} \end{pmatrix}, \quad \boldsymbol{W} = \begin{pmatrix} \boldsymbol{W}^{+} & \boldsymbol{\emptyset} \\ \boldsymbol{\emptyset} & \boldsymbol{W}^{-} \end{pmatrix}, \quad \boldsymbol{J} = \begin{pmatrix} \boldsymbol{A}^{+} & \boldsymbol{B}^{+}\boldsymbol{C}^{+} \\ \boldsymbol{A}^{-} & \boldsymbol{B}^{-}\boldsymbol{C}^{-} \end{pmatrix}.$$

5.2 Provision for the Beam Profile and the Mass Constraint

The beam profile $\boldsymbol{x}_{\text{bp}}$ can, as far as it is known and the primary particle is sufficiently short-lived, be included as a virtual measurement:

$$\boldsymbol{x}_{\text{bp}} = \boldsymbol{v} + \boldsymbol{\epsilon}_{\text{bp}} = \boldsymbol{J}_{\text{bp}} \begin{pmatrix} \boldsymbol{v} \\ \boldsymbol{z} \end{pmatrix} + \boldsymbol{\epsilon}_{\text{bp}}, \quad \mathsf{cov}(\boldsymbol{\epsilon}_{\text{bp}}) = \boldsymbol{V}_{\text{bp}} = (\boldsymbol{W}_{\text{bp}})^{-1},$$

with

$$\boldsymbol{J}_{\text{bp}} = \begin{pmatrix} 1 & 0 & 0 & 0 & 0 & 0 & 0 & 0 & 0 \\ 0 & 1 & 0 & 0 & 0 & 0 & 0 & 0 & 0 \\ 0 & 0 & 1 & 0 & 0 & 0 & 0 & 0 & 0 \end{pmatrix}.$$

This inclusion of the beam profile to constrain the result of the estimate within a certain region is especially important if the primary particle was at rest or if the directions of the secondary particles happen to be (anti-)parallel to the primary momentum. In this cases, the secondary particles fly into exactly opposite directions, such that their geometrical intersection is not well defined.

In addition, if a hypothesis for the mass of the primary particle $\bar{M} \pm \sigma_{\bar{M}}$ is available, a virtual measurement can be introduced to enforce a mass constraint:

$$\bar{M} = M + \epsilon_{\bar{M}} = \boldsymbol{J}_M \begin{pmatrix} \boldsymbol{v} \\ \boldsymbol{z} \end{pmatrix} + \epsilon_M, \quad \mathsf{var}(\epsilon_M) = \sigma_{\bar{M}}^2,$$

with

$$\boldsymbol{J}_M = \begin{pmatrix} 0 & 0 & 0 & 0 & 0 & 0 & 0 & 0 & 1 \end{pmatrix}.$$

Analogous to the previous subsection the estimate turns out to be:

$$\begin{pmatrix} \tilde{\boldsymbol{v}} \\ \tilde{\boldsymbol{z}} \end{pmatrix} = \left(\boldsymbol{J}^{\mathrm{T}} \boldsymbol{W} \boldsymbol{J} + \boldsymbol{J}_{\text{bp}}^{\mathrm{T}} \boldsymbol{W}_{\text{bp}} \boldsymbol{J}_{\text{bp}} + \tfrac{1}{\sigma_{\bar{M}}^2} \boldsymbol{J}_M^{\mathrm{T}} \boldsymbol{J}_M \right)^{-1} \left(\boldsymbol{J}^{\mathrm{T}} \boldsymbol{W} \boldsymbol{r} + \boldsymbol{J}_{\text{bp}}^{\mathrm{T}} \boldsymbol{W}_{\text{bp}} \boldsymbol{x}_{\text{bp}} + \boldsymbol{J}_M^{\mathrm{T}} \tfrac{\bar{M}}{\sigma_{\bar{M}}^2} \right).$$

5.3 Robustification

Due to the block-diagonal form of the full weight matrix $\boldsymbol{W}$, the χ^2-approach can be robustified by applying an iterative M-estimator procedure [3, 4].

Technically this is done by rewriting the objective function by a diagonalization of the weight matrices:

$$\chi^2(\boldsymbol{v}, \boldsymbol{z}) = \sum_{i=\pm} \left(\boldsymbol{\rho}^i - \boldsymbol{\sigma}^i(\boldsymbol{v}, \boldsymbol{z}) \right)^{\mathrm{T}} \boldsymbol{\Omega}^i \left(\boldsymbol{\rho}^i - \boldsymbol{\sigma}^i(\boldsymbol{v}, \boldsymbol{z}) \right)$$

with

$$\boldsymbol{\rho}^{\pm} = \boldsymbol{U}^{\pm} \boldsymbol{r}^{\pm}, \quad \boldsymbol{\sigma}^{\pm}(\boldsymbol{v}, \boldsymbol{z}) = \boldsymbol{U}^{\pm} \boldsymbol{s}^{\pm}(\boldsymbol{v}, \boldsymbol{z}),$$
$$\boldsymbol{W}^{\pm} = \boldsymbol{U}^{\pm} \boldsymbol{\Omega}^{\pm} \boldsymbol{U}^{\pm \mathrm{T}}, \quad \boldsymbol{\Omega}^{\pm} = \mathrm{diag}\left(\Omega_1^{\pm}, \ldots, \Omega_5^{\pm} \right).$$

After an initial estimation step (analogous to Eq. (5)), yielding the estimates $\tilde{\boldsymbol{v}}_0$ and $\tilde{\boldsymbol{z}}_0$, the entries of the diagonalized weight matrices $\boldsymbol{\Omega}^{\pm}$ are weighted and the estimation is repeated:

$$\Omega_k^{\pm} \longrightarrow \omega_{N,k}^{\pm} = \begin{cases} \Omega_k^{\pm} & \text{if } |\delta_{N,k}^{\pm}| \leq \frac{R}{\sqrt{\Omega_k^{\pm}}} \\ \frac{R\sqrt{\Omega_k^{\pm}}}{|\delta_{N,k}^{\pm}|} & \text{if } |\delta_{N,k}^{\pm}| > \frac{R}{\sqrt{\Omega_k^{\pm}}} \end{cases}$$

Here, N is the iteration cycle, R is the robustification constant (with a typical value between 1 and 2) and $\delta_{N,k}^{\pm} = \rho_k^{\pm} - \sigma_k^{\pm}(\tilde{\boldsymbol{v}}_{N-1}, \tilde{\boldsymbol{z}}_{N-1})$, where $\tilde{\boldsymbol{v}}_{N-1}$ and $\tilde{\boldsymbol{z}}_{N-1}$ are the estimates from the previous iteration step. The iteration stops if the improvement of the objective function becomes negligible, i.e. if $\Delta\chi^2 = |\chi^2(\tilde{\boldsymbol{v}}_N, \tilde{\boldsymbol{z}}_N) - \chi^2(\tilde{\boldsymbol{v}}_{N-1}, \tilde{\boldsymbol{z}}_{N-1})| < \epsilon_{\chi^2}$.

This procedure is also possible in the presence of the mass constraint and the inclusion of the beam profile, since the corresponding virtual measurements are independent from each other and the residuals $\boldsymbol{r}^{\pm}$.

6 Results

The concept described above has been implemented in the CMS reconstruction and analysis framework CMSSW [5]. The decays of primary particles into muon-antimuon pairs and the corresponding signal in the Tracker [6, 7] have been fully simulated. Two samples, one with 50,000 Z^0-bosons and another one with 25,000 J/Ψ-mesons as primary particles, have been produced to allow for a comparison between the two cases of loose and tight mass constraint. The primary momenta were uniformly distributed between 50 GeV and 100 GeV in the Z^0-sample and between 100 GeV and 150 GeV in the J/Ψ-sample, resulting in a rather broad spectrum of secondary

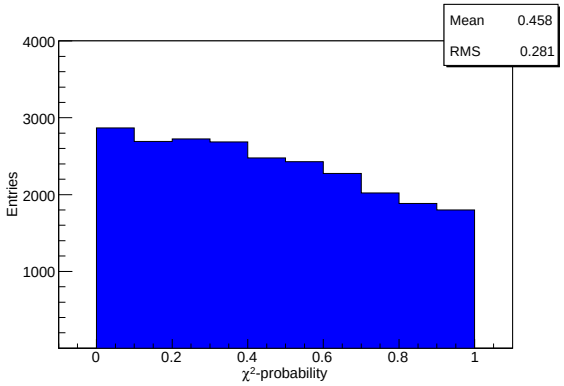

Figure 3: χ^2-probability of the kinematical fit (including the beam pofile and mass constraint).

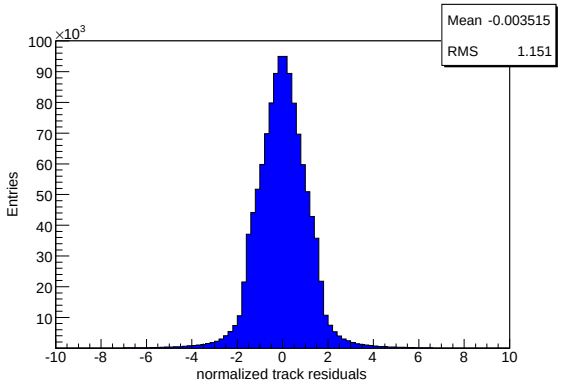

Figure 4: Normalized residuals of the repropagated trajectories.

momenta from the region of a few GeV up to the kinematic limit in both cases. The positions of the decay vertices were generated randomly by drawing from Gaussians with variances according to the expected beam profile ($\sigma_x = \sigma_y = 15\,\mu$m, $\sigma_z = 5.3$ cm). The resulting tracks covered the whole sensitive η-range of the Tracker.

For the reconstruction of the tracks the standard algorithms were utilized [8]. The resulting estimates on the track parameters were used for a geometrical vertex fit to obtain $\boldsymbol{v}_0$ and to compute the expansion point $\boldsymbol{z}_0 = (\boldsymbol{p}_0, \theta_0, \phi_0, M_0)^{\mathrm{T}}$ for the susbsequent kinematical fit. The provisional momentum of the primary particle $\boldsymbol{p}_0$, estimated to be simply the sum of the tracks' momenta at their point of closest approach towards $\boldsymbol{v}_0$, was also used to obtain a first guess of the parameters defining the Lorentz transformation from the lab-frame to the rest-frame of the two-body decay. By transfoming (at least one of) the single-track momenta into the rest-frame, the parameters θ_0 and ϕ_0 were computed. The invariant mass of the tracks was used for the parameter M_0.

For all cases the robustified procedure (with $R = 1$ and $\epsilon_{\chi^2} = 10^{-2}$), including the proper mass constraint and the beam-profile, was used. The results from the kinematical fit as well as the results from the standard reconstruction (a least-squares vertex fitter implemented in the Kalman filter formalism using the beam profile as external prediction) have been compared to the simulated truth.

6.1 Principal functionality

The principal functionality has been tested on the $\mathrm{Z}^0 \longrightarrow \mu^+\mu^-$ sample. Figure 3 shows the χ^2-probability distribution of the estimates, or more strictly speaking, the distribution of $1 - F_{n=5}\left(\chi^2(\tilde{\boldsymbol{v}}, \tilde{\boldsymbol{z}})\right)$. $F_n(x)$ is the cumulative χ^2-distribution function with n degrees of freedom and $\tilde{\boldsymbol{v}}$ and $\tilde{\boldsymbol{z}}$ are the final estimates of the iterative M-estimator procedure. The resulting flat, almost uniform distribution is a strong indication that, despite the high non-linearity of the decay-model and the need of a twofold linearization step, the linear model is appropriate to parameterize and estimate the properties of two-body decays.

Furthermore, the proper representation of both single-tracks through the proposed set of parameters is demonstrated in Figure 4, where the normalized residuals between the observed measurements $\boldsymbol{m}$ and the reference trajectory $\boldsymbol{f}(\tilde{\boldsymbol{v}}, \tilde{\boldsymbol{z}})$ are shown, i.e. the distribution of $(m_i - f_i)/\sqrt{V_{ii}}$. The highly non-gaussian shape of the distribution is mostly due to the fact that the measurements of the local v-coordinate, i.e. along the direction of the strip of the sensitive modules, are uniformly distributed.

6.2 Impact of the Mass Constraint

Tables 1 and 2 show the results for the decays of J/Ψ and Z^0. These two examples clearly demonstrate the impact of the particle width on the precision of the estimated parameters. Whereas the mass of the J/Ψ ($\sigma_{\mathrm{J}/\Psi} = 91.0$ keV) is clearly defined, the width of the Z^0 is much larger ($\sigma_{\mathrm{Z}^0} = 2.5$ GeV). As can be seen, this distinct constraint restricts not only the resulting value of the fitted mass, but also improves the estimate as a whole, since the mass is a crucial parameter for the kinematics.

	σ_{SR} [μm]	σ_{KF} [μm]	σ_{KF}/σ_{SR}
Δv_x	25.89	13.36	0.52
Δv_y	26.91	13.33	0.50
Δv_z	119.0	139.0	1.17

	σ_{SR} [GeV/c]	σ_{KF} [GeV/c]	σ_{KF}/σ_{SR}
Δp_x	1.034	0.481	0.47
Δp_y	1.024	0.516	0.50
Δp_z	2.206	1.025	0.46

	σ_{SR} [GeV/c^2]	σ_{KF} [GeV/c^2]
Δm	0.066	$9.074 \cdot 10^{-5}$

Table 1: Comparison of the results from the kinematical fit (KF) and the standard reconstruction (SR) for a sample of 25.000 simulated $J/\Psi \longrightarrow \mu^+\mu^-$ decays (no misalignment applied). Shown are the r.m.s errors of the estimated quantities w.r.t. to their true values.

	σ_{SR} [μm]	σ_{KF} [μm]	σ_{KF}/σ_{SR}
Δv_x	12.15	11.04	0.91
Δv_y	12.41	11.22	0.90
Δv_z	33.06	35.65	1.08

	σ_{SR} [GeV/c]	σ_{KF} [GeV/c]	σ_{KF}/σ_{SR}
Δp_x	0.762	0.701	0.92
Δp_y	0.737	0.679	0.92
Δp_z	1.003	0.934	0.93

	σ_{SR} [GeV/c^2]	σ_{KF} [GeV/c^2]	σ_{KF}/σ_{SR}
Δm	0.940	0.858	0.91

Table 2: Comparison of the results from the kinematical fit (KF) and the standard reconstruction (SR) for a sample of 50.000 simulated $Z^0 \longrightarrow \mu^+\mu^-$ decays (no misalignment applied). Shown are the r.m.s errors of the estimated quantities w.r.t. to their true values.

	σ_{SR} [μm]	σ_{KF} [μm]	σ_{KF}/σ_{SR}
Δv_x	22.76	16.92	0.74
Δv_y	23.66	17.34	0.73
Δv_z	76.93	82.93	1.08

	σ_{SR} [GeV/c]	σ_{KF} [GeV/c]	σ_{KF}/σ_{SR}
Δp_x	3.021	2.426	0.80
Δp_y	2.859	2.280	0.80
Δp_z	2.795	2.158	0.77

	σ_{SR} [GeV/c^2]	σ_{KF} [GeV/c^2]	σ_{KF}/σ_{SR}
Δm	2.860	2.265	0.79

Table 3: Comparison of the results from the kinematical fit (KF) and the standard reconstruction (SR) for a sample of 50.000 simulated $Z^0 \longrightarrow \mu^+\mu^-$ decays (with applied misalignment). Shown are the r.m.s errors of the estimated quantities w.r.t. to their true values.

6.3 Performance in the Presence of Misalignment

In the case of a misaligned Tracker, the benefit from exploiting the kinematics becomes greater, even in the case of weak mass constraints. Table 3 shows the gain of precision compared to the standard reconstruction in the presence of misalignment as expected at the start-up phase of the CMS experiment [9]. Though the expected misalignment is accounted for in the standard track reconstruction by increased position errors of the measurements, the kinematical fit improves the estimate still by approximately 20%.

7 Conclusions

A parametrization useful for describing and estimating the kinematic properties of two-body decays has been derived. This parametrization also allows to represent the trajectories of the secondary particles in a proper and concise way, reusing concepts usually found in tracking and vertexing. Therefore the time and effort for the

implementation of this procedure is rather small and less error-prone.

References

[1] A. Strandlie, W. Wittek, *Propagation of Covariance Matrices of Track Parameters in Homogeneous Magnetic Fields in CMS*, CMS NOTE 2006/001.

[2] R. Frühwirth et al., *Data Analysis Techniques for High-Energy Physics*, Cambridge University Press, 2000.

[3] Frank R. Hampel et al., *Robust Statistics*, Wiley, New York, 1986.

[4] R. Frühwirth et al., Comput. Phys. Commun. 96:189, 1996.

[5] The CMS Reconstruction and Analysis Framework. See `http://cms.cern.ch/iCMS`.

[6] The CMS Collaboration, *The Tracker Project Technical Design Report*, CERN/LHCC 98-6.

[7] The CMS Collaboration, *Addendum to the Tracker TDR*, CERN/LHCC 2000-016.

[8] W. Adam et al., *Track reconstruction in the CMS tracker*, CMS NOTE 2006/041.

[9] I. Belotelov et al., *Simulation of Misalignment Scenarios for CMS Tracking Devices*, CMS NOTE 2006/008.